12

Deposition and Characterization of Platinum and Palladium Nanoparticles on Highly Oriented Pyrolytic Graphite

Nora Elizondo et al.*,
Facultad de Ciencias Físico-Matemáticas,
México

1. Introduction

Nanostructured transition metal nanoparticles are of great interest from both fundamental and practical view points because of the quantum size effect, which is derived from the dramatic reduction of the number of free electrons. [Halperin, 1986; Schmid, 1994] Volokitin et al. have found that the quantum size effect strongly affected the thermodynamics of the metal nanoparticles. [Volokitin et al., 1996; Colvin et al., 1994; Andres et al., 1992]

Platinum is considered one of the best electrocatalyst for low temperature reactions in a H_2/O_2 fuel cell. Palladium is an element of the platinum group metals and it has similar chemical properties. Nanoparticles(Nps) are of great interest because of the modification of properties observed due to size effects, modifying the catalytic, electronic, and optical properties of the monometallic Nps. Interest in platinum Nps derives mostly from the importance of highly dispersed platinum and palladium in catalysis. [Colvin et al., 1994; Andres et al., 1992] They have been concretly applied to catalysts[Lewis, 1993] for hydrogenation of olefins and dienes,[Hirai et al., 1986; Teranishi, 1996] hydration of acrylonitrile to acrylamide,[Toshima & Wang 1994] photogeneration of hydrogen from water,[Bard, 1980] and reduction of carbon dioxide,[Willner et al., 1987; Toshima et al.,1995]

Donald H. Galván[3], Lorena Álvarez-Contreras[4], Ran Tel-Vered[5], Arquímedes Cruz-López[2], Ricardo Obregón[1], Sergio Belmares-Perales[1], Manuel García-Méndez[1], Odilón Vázquez-Cuchillo [2] and Antonio A. Zaldívar[2]

[1]*Facultad de Ciencias Físico-Matemáticas, México*
[2]*Facultad de Ingeniería Civil,*
Universidad Autónoma de Nuevo León, San Nicolás de los Garza, N. L., México
[3]*Centro de Nanociencias y Nanotecnología,*
Universidad Nacional Autónoma de México, Ensenada, México
[4]*Departamento de Química de Materiales,*
Centro de Investigación en Materiales Avanzados, S. C., Chihuahua, México
[5]*Institute of Chemistry, The Hebrew University of Jerusalem, Jerusalem, Israel*

the catalytic activity and selectivity being strongly affected by the particle size. To investigate the physical and chemical properties of metal nanoparticles, especially the size-dependent properties, precise control of the particle size is essentially required. Moreover, the precise control of particle size is also required for the organization of metal nanoparticles.[Teranishi et al., 1997; Reetz et al.,1997]

It has been found from mass spectral studies that the binding energies of metal nanoparticles consisting fewer than ca. 1000 atoms vary periodically due to the quantum size effect.[Sugano, 1991; Katakuse, 1994] This phenomenon was first found by Knight et al.[Knight et al., 1984] through experiments involving Na nanoparticles. This suggests the discontinuous existence of nanoparticles having certain stable structures. Therefore, a synthetic technique is required to produce the nanoparticles with any sizes within a few angstroms in standard deviation.

The usual synthetic technique for making such nanoparticles involves chemical or electrochemical reduction of metal ions in the presence of a stabilizer such as linear polymers, [Teranishi, 1996; Toshima et al., 1991, 1995; Hirai et al., 1985; Henglein, 1993; Bradley et al., 1991; Hirai, 1979] ligands, [Schmid, 1992; Poulin et al., 1995; Amiens, 1993] surfactants, [Toshima & Takahashi, 1992; Yonezawa et al., 1995; Esumi et al., 1995; Leff et al., 1995]

An "ideal" model system for investigating a particle size effect in electrochemical reactions- such as the methanol oxidation and oxygen reduction reactions- would possess all of the following characteristics: (1) Platinum nanocrystals should be size and shape monodisperse. (2) Nanocrystals should be dispersed on, and electrically connected to, a technologically relevant support surface that facilities spectroscopic characterization of the particles and of adsorbed intermediates. For many electrocataysis reactions the preferred support material is graphite. (3) Individual platinum particles on this support should be well-separated from one another. (4) The structure of the platinum nanocrystals on the support surface should be accessible both before and following the involvement of these particles in the catalytic process of interest. (5) Supported and platinum Nps should be stable for days [Zoval et al., 1996; Thomas et al.,1996; Bronstein et al., 2000; Han et al., 1998; Freelink et al. 1995].

Control of particle size by using the ligands has been extensively studied, [Schmid et al., 1992] many shell-structured nanoparticles being synthesized, such as 2-shell Au,[Schmid et al., 1984] 4-shell Pt,[Schmid et al., 1989] and 5, 7, and 8-shell Pd[Vargaftik et al.,1991; Schmid, 1988; Schmid et al.,1993] nanoparticles. When a linear polymer is used as a protective agent, modification of the functional groups can offer a specific reaction field around the metal nanoparticles that promotes the catalytic activity of the nanoparticles and may change the electronic structures of the metal nanoparticles. Ahmadi et al. succeeded in controlling the shape of Pt nanoparticles by using sodium polyacrylate as a capping polymer.[Ahmadi et al., 1996] We have controlled the size of Pt and Pd nanoparticles by using poly (vinylpyrrolidone) (PVP) and succeeded in their two dimensional organization. Thus, linear polymers have great potential as protective agents for nanoparticles and as stabilizers and ethylenglycol as a reductor.[Park et al., 2008; Cao, 2004] Such procedure yield different morphologies and sizes of metal Nps (including platinum and palladium).[Teranishi & Miyake, 1998] The interaction between PVP and metal precursors has effect on the formation of the colloidal metal nanoparticles. Strength of the interaction between PVP and metal nanoparticles has direct

influence on the stability and the size of the PVP-stabilized metal nanoparticles. Therein, species of the metal precursors and amount of the stabilizer are main factors on the strength of the interaction.[Wei-xia, 2008]

The polyol method has been reported to produce the platinum and palladium nanoparticles as the final product,[Yonezawa & Toshima, 1993],[Kan et al., 2003; Sanchez-Ramirez, 2001; Viau et al., 2001] easily changing surface modifiers. This technique does not require an additional reducing agent since the solvent by itself reduces the metallic species.[Tekaia-Elhsissen et al., 1999; Bonet et al., 1999] However, besides the stoichiometry and order of addition of reagents in the synthesis process, one of the most important[Turkevich et al., 1951] parameters in the preparation is the temperature. Modifications in temperature influence the reaction by changing the stabilization of the complexes formed between Pt and Pd respectively with the surface modifiers, e.g., PVP, and the nucleation rate of the reduced metallic atoms.[Garcia-Gutierrez et al., 2008]

In this chapter, a colloidal method of synthesis has been proposed to obtain metallic Nps; the polyol method has been reported to produce small Nps as the final product. [Alvarez et al., 1997; Henglein et al., 2000; Grabar, 1995; Baker, 1996]

The gas-phase method of platinum and palladium salt particles disposed on a graphite surface by H_2 was used in this work. This method has the potential to yield nanocrystals that are disposed in direct contact with a substrate surface. [Bartolomew & Boudart, 1972]

In this work we describe an electrochemical method for preparing dispersions of platinum and palladium nanocrystals on a graphite basal plane surface involving the pulsed potentiostatic deposition of platinum from dilute $PtCl_6^{2-}$ using large overpotentials ($E_{overvoltage} \approx 500$ mV) and by overpotential deposition also with higher Pd^{2+} concentrations in solution. [Reetz et al., 1992; Allongue & Souteyrand,1992 ; Cachet et al., 1992; Diculescu et al., 1992]

A novel approach to characterize this kind of particles is based on the use of HAADF technique, in a high resolution transmission electron microscope (HRTEM), which allowed us the observation of the elements due to atomic number, densities, or the presence of strain fields due to differences in lattice parameters, structure, the presence of surfactants or any other surface modifier besides the size of the particle. [Williams & Carter, 1996]

The interaction between metal nanoparticles and substrate surfaces has long attracted attention. This is because of underlying interests in understanding (1) the behavioral transition from atomic to bulklike properties, as a function of nanoparticle size, (2) the effect of size-dependent electronic structures in heterogeneous catalysis, (3) the dimensionally controlled fabrication of supported nanoparticles, (4) thin film deposition onto heterogeneous surfaces and (5) the adhesion associated with interfacial interactions. Studies have indicated that the evaporation, sputter, and electrochemical depositions of Pt and Pd all lead to particle formation on such substrates, due to both a lack of substrate wetting and relatively weak interfacial interactions. [Yang et al., 2006]

The HOPG is described as consisting of a lamellar structure the freshly cleaved surface consists of atomic steps and steps of several or dozens of atomic layers. The crystallographic planes do have a definite structure and the height of a single step is 0.34 nm. [Pauling,

1960]The Moiré patterns and rotations between the first and second layers of HOPG in the direction perpendicular to the basal plane by effect of heating Pt Nps on HOPG (in H_2 flow) were observed. [Williams & Carter, 1996; Pauling, 1960; Beyer et al., 1999]

2. Experimental section

The polyol method was followed to obtain platinum and palladium metallic Nps passivated with poly(vinylpyrrolidone) (PVP). Hexachloroplatinic (IV) acid (H_2PtCl_6) hydrate (99.99%), Palladium Chloride(II) and poly (N-vinyl-2-pyrrolidone) (PVP-K30, MW = 40000) were purchased from Sigma Aldrich, and 1,2-ethylenediol (99.95%) was purchased from Fischer Chemicals; all the materials were used without any further treatment.

A 0.4 g sample of Poly (N-vinyl-2-pyrrolidone) (PVP) was dissolved in 50 mL of 1,2-ethylenediol (EG) under vigorous stirring, heating in reflux, until the desired temperature was reached (working temperatures ranged from 100 °C to 190 °C in increments of 10 °C). For the Pt and Pd metallic Nps, a 0.1 mM EG-solution of the metal precursor was added to the EG-PVP solution, with continuous agitation for 3 h in reflux. When preparing the Pt and Pd metallic Nps, the following criterion was used: after complete dissolution of PVP in EG, 2 mL of an EG solution of H_2PtCl_6 (0.05 M) and $PdCl_2$ was added to the EG-PVP solution in a period of 1 h. The reaction was carried out for 3 h at constant temperature. For this work the Pt and Pd Nps presented the smaller average size for a synthesis performed at 130 °C. These Pt and Pd Nps in a solution of ethanol were impregnated on HOPG and dried in a oven at 80°C.

The Pt and Pd Nps preparation on HOPG by direct reduction of Platinum and Palladium salts in H_2 flow on HPOG (the gas phase method) consisted in the partial oxidation of the support in a muffle furnace at 600°C for 24 hours. Then the impregnation of preoxidized HOPG with chloroplatinic acid and palladium chloride solutions respectively in a four to one mixture of benzene to ethanol (absolute). The metal concentrations were adjusted to produce the desired total metal loading (10 Wt % Pt and 10 Wt % Pd). The amount of solvent was fixed using 50 mL/g of HOPG. A mixture of salt solution and HOPG was shaken while nitrogen was bubbled through the suspension at flow rate of 200-500 mL/min until to solution evaporated to dryness, i.e., after 40-60 h for a 10 g sample in 500 mL of solution.

The samples prepared by these methods (Pt and Pd Nps on HOPG) were heated in a H_2 flow at a temperature range from 450 ^oC to 1000 ^oC during time intervals from 2h to 5 h. Samples were then exfoliated with a scotch tape for TEM observation.

Pt and Pd Nps were electrochemically deposited on a highly oriented pyrolytic graphite (HOPG, grade-1) which was obtained from SPI Supplies (West Chester, PA). In the case of Platinum depositions were carried out by immersing the potential in which electroless platinum deposition was not observed), followed by stepping the potential of the graphite surface to a deposition potential of -0.6 V, for 100 ms. Following the application of the deposition pulse, the electrode potential was stepped back to 0.2 V, and the working electrode was removed from the plating solution. All electrochemical experiments were performed using a CH Instruments potentiostat model CHI 900B (CH Instruments, Austin, TX). A platinum coil (d=0.5 mm) and a Hg/Hg_2SO_4 were used as the counter and reference electrodes, respectively.

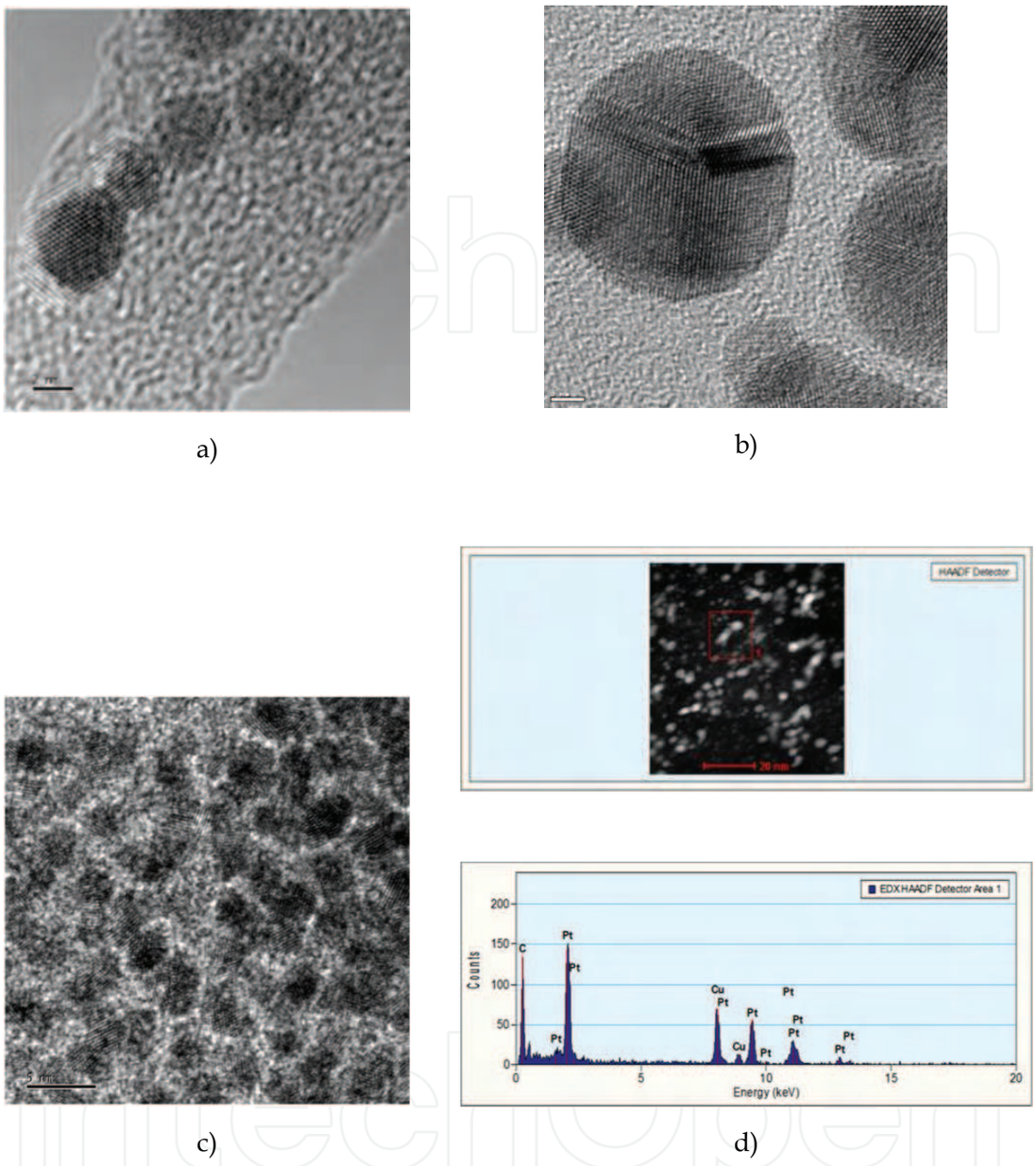

Fig. 1. A microscopy images by HRTEM, show metallic Nps synthesized by polyol method at: a) platinum(2 nm length bar), b) palladium(2 nm length bar), c) platinum well dispersed synthesized at 145 °C(5 nm length bar), and d) HAADF shows of Pt nanoparticles and EDX HAADF analyze of Pt nanoparticles(20 nm length bar), peaks for Cu and C are from the grid used.

The Pt and Pd Nps on HOPG for the electron microscopy analysis were prepared over lacey carbon TEM grids. HRTEM images were taken with a JEOL 2010F and a Titan FEI microscopes. HAADF images were taken with a JEOL 2010F microscope in the STEM mode, with the use of a HAADF detector with collection angles from 50 mrad to 110 mrad.

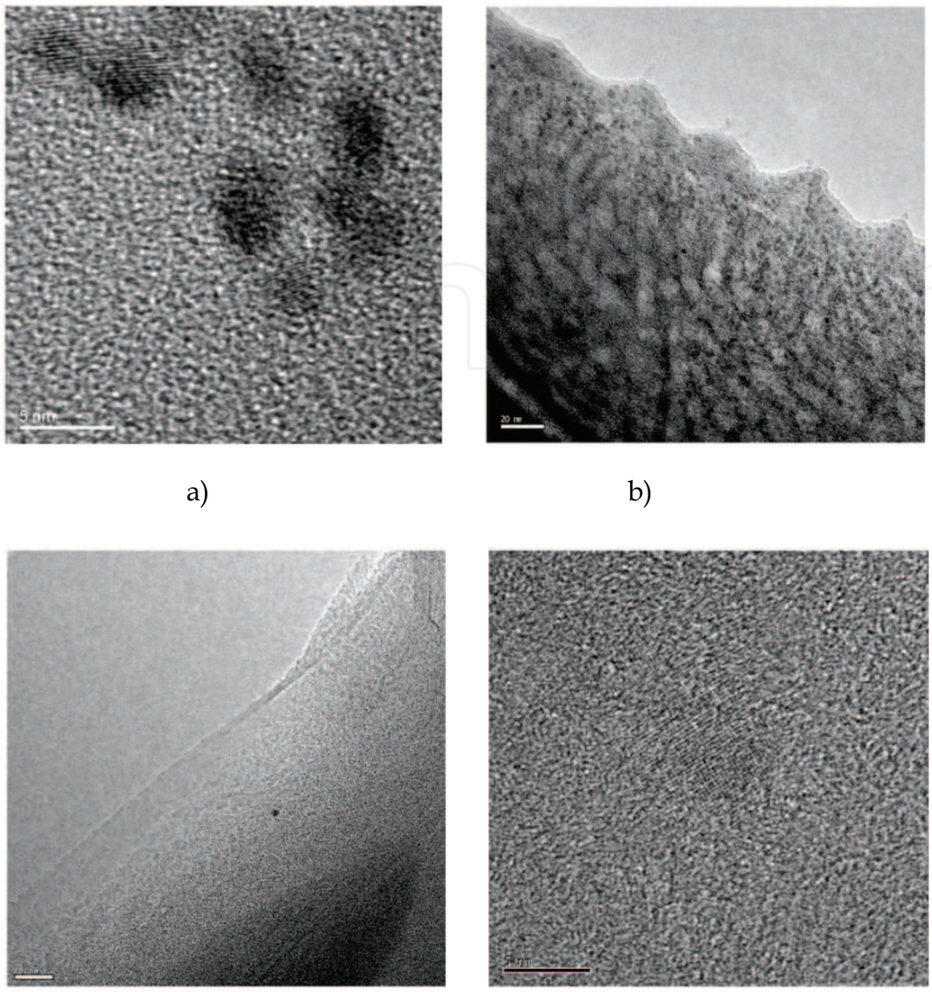

a) b)

c) d)

Fig. 2. HRTEM images of: a) of Pt Nps on HOPG synthesized by polyol heated in H_2 flow at 450ºC(5 nm length bar), b) Pt nanoparticle synthesized on HOPG by the electrochemical method(20 nm length bar), c) Pd Np synthesized by polyol on HOPG(20 nm length bar), and d) Pt nanoparticle synthesized on HOPG graphite by direct reduction of chloroplatinc acid impregnated on HOPG and heated in H_2 flow at 950 ºC(5 nm length bar).

3. Electronic properties of bilayered graphene with platinum and bilayered graphene with palladium atoms on one of the layers

High resolution transmission electron microscopy analysis of two-layered graphene yielded Moiré patterns induced by Pt atoms/clusters located at the top of one of the layers, which induce rotation between planes. The rotations measured vary between 3 and 5 degrees. Theoretical analysis was performed using an extended Hückel tight-binding scheme on two-layered graphene with either containing two carbon atom vacancies or with two Pt atoms, with a cluster of 6 Pt atoms or with a cluster of 13 Pt atoms located at the top of one of the graphene layers. In most of the cases, the system remains semi metallic, except when a

cluster of 6 Pt atoms was located on the surface of one of the graphene layers. For this case, the system behaves as a semi conductor with an energy gap $E_g \sim 0.05$ eV.

We have also investigated the scenario of graphene when irradiated with high energetic protons and latter decorated with Pd atoms on one of the layers. Theoretical analysis were performed on graphene 2L (two layers) with vacancies (carbon 3 and 13), graphene 2L with vacancies and intercalated in between the two carbon layers, graphene 2L with the vacancies intercalated and subsequently with two Pd atoms on one of the layers (called surface), and last but not least, graphene 2L with vacancies intercalated and decorated with six Pd atoms on the surface. For the three cases enunciated formerly, energy bands were performed and provided information about the metallic behavior, showing more metallic character for the first case, while less metallic behavior for the second one. Moreover, for graphene 2L with vacancies and intercalated with six Pd atoms on the surface showed a mini gap (between the Conduction and Valence Bands) of the order of 0.02 eV and manifesting semiconductor behavior.

4. Theoretical analysis

The calculations reported in this work, have been carried out by means of the tight-binding method [Whangbo & Hoffmann, 1978], within the extended Hückel [Hoffmann, 1963].framework using YAeHMOP (Yet Another extended Huckel Molecular Orbital Program) computer package with f-orbitals.[Glassey et al., 1999] It is good to stress that the extended Hückel method is a semi empirical approach for solving Schrödinger equation for a system of electrons, based on the variational theorem. In this approach, explicit electron correlation is not considered except for the intrinsic contributions included in the parameter set. Furthermore, neither the relativistic contributions form the Dirac electrons were considered, except that they indirectly appear in the parameter set which were obtained from S. Alvarez et al.[Alvarez, 1993] or from the most accurate *ab initio* calculations. More details about the mathematical formulation of this method have been described elsewhere.[Galván, 1998]

Calculations were performed on a system selected as a repeated cluster originated from a super cell. The super cell was generated from an infinite single sheet of carbon atoms, as depicted in Fig. 3, which aroused from crystalline graphite using the following primitive vectors: a = 2.456 Å, c = 6.696 Å, space group 186.[Hull, 1917; Hoffmann & Wilm, 1936]

The structure for graphene was made of two hexagonal layers located one at the top of the other layer separated by a distance of 3.348 Å apart. In order to make the calculations easier, a new cluster smaller than the original could be constructed. This new cluster is made-up of 40 carbon atoms in single layer, and then duplicates the second layer with a similar number of atoms separated by a distance of 3.348 Å. apart. For the graphene with platinum atoms at the top of the layer, considered as the surface, two Pt atoms were located at the center of the hexagonal rings, while the second Pt atom was located in an adjacent hexagonal ring. We also investigated the existence of vacancies created when two carbon atoms were removed from the original structure. In order to extend our investigation further whenever the number of Pt atoms was increased to a 6 Pt atoms cluster which was located it on the top one of the graphene layers. Furthermore, in order to complete to a more *realistic* problem, a cluster made of 13 Pt atoms previously optimized, was located at top the graphene layer

with vacancies, and latter one of the graphene layers was rotated by 3 and 5 degrees with respect to the other layer.

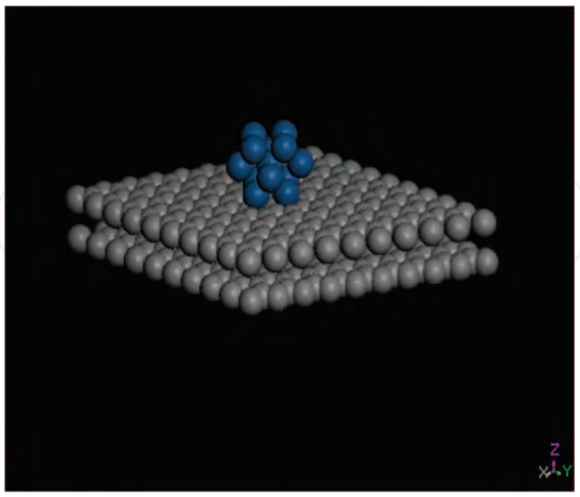

Fig. 3. Inifinite hexagonal arrays of carbon atoms used in order to generate the honeycomb structure for graphene. Grey balls are carbon atoms while blue balls correspond to Pt atoms.

Atomic parameters for carbon, platinum and palladium atoms used through the calculations were obtained from Alvarez et al.[Alvarez, 1993] and provided in Table 1.

Atom	**Orbital**	$\mathbf{H_{ii}}$	ς_{i1}	$\mathbf{C_1}$	ς_{i2}	$\mathbf{C_2}$
C	2s	-21.40	1.62			
	2p	-11.40	1.62	0.0000	0.0000	0.0000
Pt	6s	-9.07	2.55			
	6p	-5.47	2.55			0.5513
	5d	-12.59	6.01	0.6334	2.6960	
Pd	5s	-7.32	2.19			
	5p	-3.75	2.15			
	4d	-12.02	5.98	0.5535	2.613	0.6701

Table 1. Atomic parameters used in the Extended Hückel tight-binding calculations, H_{ii} (eV) and ς (Valence orbital ionization potential and exponent of Slater type orbitals). The d-orbitals for Pt and Pd are given as a linear combination of two Slater type orbitals. Each exponent is followed by a weighting coefficient in parentheses. A modified Wolfsberg-Helmholtz formula was used to calculate H_{ij}.[Wolfsberg & Helmholtz, 1952]

Experimental lattice parameters instead of optimized values were used searching for a best matching of our theoretical results with the available experimental information. In order to explain the diffraction patterns in 2-L rotated graphene with vacancies with two Pt atoms and latter on with 6 Pt cluster located on one of the layers, we shall proceed with the same kind of reasoning as we proceeded in different systems like crystalline graphite and dichalcogenides, when these systems were irradiated with different sources like, electrons γ-rays, etc. as reported by our group.

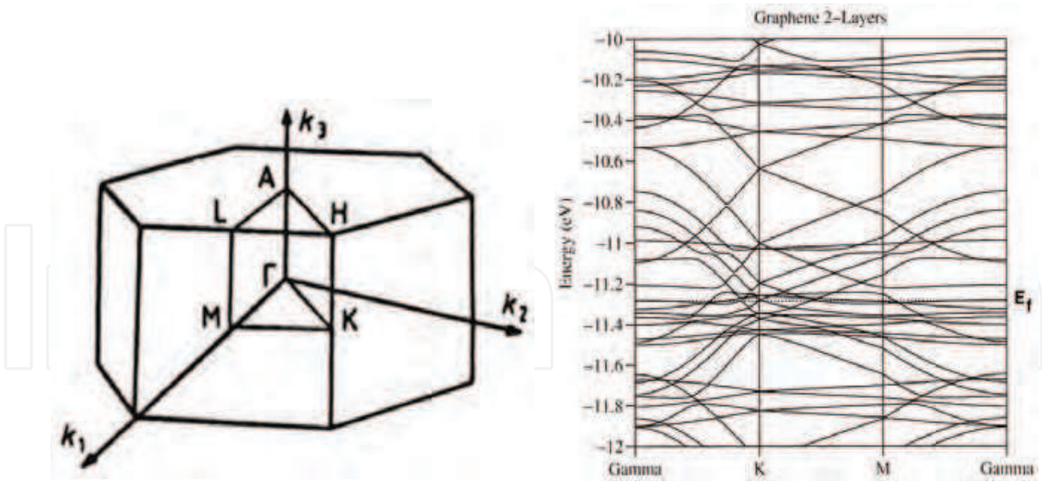

Fig. 4. Energy bands for graphene 2-L. The inset depicts the Wigner-Seitz cell for a hexagonal configuration.

Band structure calculations for 2-L graphene, graphene with two carbon vacancies, graphene with vacancies and two Pt atoms located on the top of one of the layers (from now on we shall call it surface), graphene with vacancies and a cluster of 6 Pt atoms located on the surface rotated by 3 degrees then rotated by 5 degrees were calculated using 51 k-points for each case, and sampling the First Brillouin zone (FBZ) as depicted in figure 4, figures 5 (a) to (b) and 6 (a) to (b), respectively.

First, notice that for graphene 2-L, the average energy is -5622.2462 eV and looking at Fig. 4, the system has a metallic behavior due that many degenerate bands overlap at the E_f.

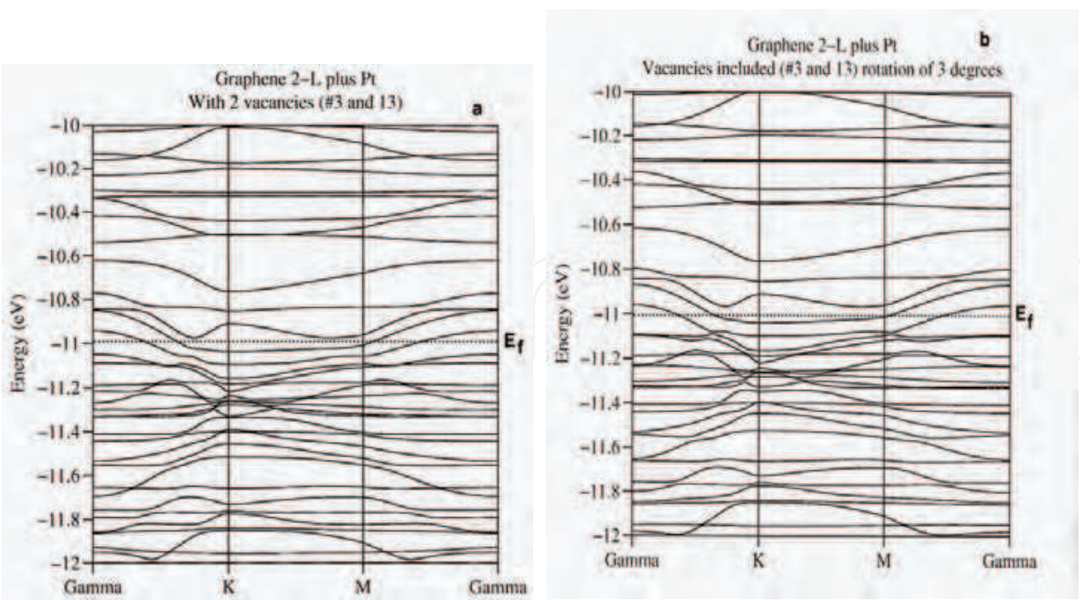

Fig. 5. (a) to (b) Band structure calculations for graphene 2-L plus two Pt atoms at the surface with two vacancies, graphene 2-L with 2 vacancies and two Pt atoms located at the surface when a rotation of 3 degrees was applied.

In order to answer the question regarding to what will it happen to the graphene when two platinum atoms were located on the surface of one of the platinum layers? Notice that the average energy for the new system changes from -5622.2462 eV to -5888.8251 eV respectively. At the same time, the E_f slightly changes due to the extra electrons provided by each Pt atom, Fig. 5 (a). Moreover, E_f is shifted to more negative values and due that Pt d-orbitals, which are located in the vicinity of the E_f, the system tends to behave as a semi metal. Then a rotation of 3 degrees is applied to one of the layers (the surface layer), as depicted in Fig. 5 (b), the average energy changes from -5888.8251 eV to -5888.8727 eV.

Notice a similar energy, except a small difference is noted after the decimal point. This means that the small perturbation was not enough to change the original system to another state and the space group remains the same as the unrotated one. On the other hand, when rotations of 4 and 5 degrees were applied to one of the planes, the average energy changes from -5888.8251 eV to -5891.6542 eV and -5889.3285 eV respectively, the perturbations applied were too severe that the systems obtained were different because the original symmetry was broken hence we have an unfavorable state.

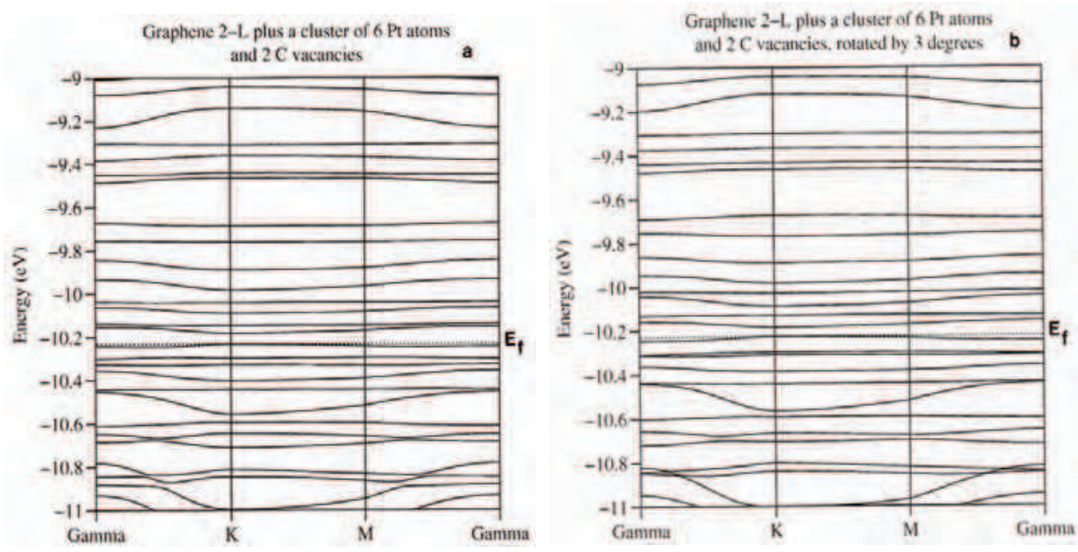

Fig. 6. (a) to (b) Band structure calculations for graphene 2-L , two carbon vacancies and a cluster of 6 Pt atoms located at the surface, graphene 2-L with vacancies and a cluster of Pt atoms located at the surface, a rotation of 3 and five degrees rotation was applied to the surface.

Figures 6 (a) to (b) yield the information regarding to graphene with two carbon vacancies (the order of vacancies considered through the calculations were of 2.5%) and a cluster of six Pt atoms located at the surface of one of the layers. Notice that the average energy of the system without rotation is of the order of -6246.7627 eV. The difference obtained, when compared to graphene with two C vacancies and two Pt atoms located at the surface of one of the layers, is attributed to the extra Pt atoms, which promotes that the new system tends to be a semiconductor with a forbidden energy gap $E_g \sim 0.05$ eV between the VB and CB, as depicted in Fig. 6 (a). When rotation in between layers of three degrees is applied, the average energy obtained was -6246.9018 eV similar to the unrotated case. The space group remains the same as the unrotated case, meaning that the rotation by three degrees is favored.

On the other hand, when a rotation of 5 degrees is applied to the surface layer, an average energy of -6247.2204 eV was obtained. Indicating that the perturbation applied was enough to place the system into another different state than the original one; we observe that the energy bands reflect a semi conductor behavior for the system with an $E_g \sim 0.05$ eV.

Moreover, when the 13 Pt atom cluster was located at the top (surface) of one of the layers a different scenario was observed. The total average energy for the new system change to -7119.7938 eV and the energy bands provide indication of semi metallic behavior. Furthermore, when a 3 degree rotation was applied to the surface, the average energy changes to -7120.0174 eV. The fact that the average energy changes (when compared to the un rotated case), provide an indication that the rotation applied was severe enough as to break the original symmetric group ending into another group, although the semi metallic behavior is still present. This behavior could be attributed to the stiffness provided to the material created when the cluster was located at the top surface layer.

We have been able to explain the original diffraction patterns observed in graphene with Pt atoms decorated on the surface, these are the direct result of a rotation of layers of the carbon honeycomb network. The rotations of 3 to 5 degrees are favored.

If the system is going to be a good promoter of the catalytic activity, the graphene (2-L) with vacancies and two Pt atoms on the surface, present metallic behavior, being the 3 to 5 degrees rotation the states which are favored.

On the other hand, when graphene and Pd case was analyzed, we proceeded in the following way: To prepare our theoretical *sample*, an infinite hexagonal honeycomb arrangement of carbon atoms were considered as depicted in Fig. 7 (a). To make the calculations simpler, a graphite single sheet made of 40 carbon atoms as depicted in Fig. 7 (b) were considered and in which 2 carbon atoms (3 and 13) were removed, as it would be a likely case of the effect of the proton irradiated beam on the sheet of carbon atoms. Moreover, these two carbon atoms were located at a distance of 1.67 Å (half way between the two layers) from the top layer and intercalated in between the second sheet, following a duplication of the second sheet and constructed of 40 carbon atoms in the AA configuration in order to create the two layers of graphene. The former configuration was made with the purpose of simulating a *real* scenario if -graphene 2Lwere subjected to proton irradiation.

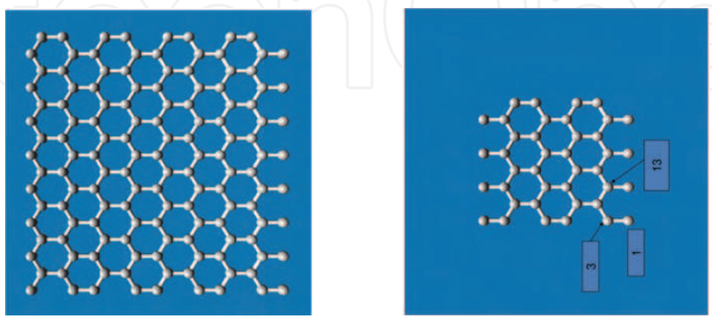

a) b)

Fig. 7. (a) Super cell generated from an infinite single sheet of carbon atoms. (b) A cell made out of 40 carbon atoms per layer was constructed.

A natural candidate to generate magnetism in coated graphene is Pd, due to its very polarizable bands. Furthermore, Pd is not intrinsically magnetic due to its close shell configuration ($[Kr]^{36}4d^{10}$) of the d orbitals. Although, in bulk, the s and d bands of Pd hybridize and exhibit Pauli paramagnetism with a high density of states in the vicinity of the Fermi level.

With these considerations in mind, our goal is to consider graphene two layers (2L) with two vacancies (carbon 3 and 13) intercalated in between the two layers and decorated with Pd atoms on one of the layers, in order to inquire about the changes occurred in the electronic and magnetic properties.

Band structure calculations for graphene two layers with vacancies (carbons 3 and 13), from now on indentified as graphene 2L (a), graphene two layers with two vacancies and intercalated in between the two layers, identified as graphene 2L (b), graphene two layers with vacancies and intercalated between the two layers with two Pd atoms located at the top of one of the layers (called surface), identified as graphene 2L (c) and last but not least, graphene two layers with vacancies intercalated between the two layers with 6 Pd atoms located in the center of six hexagons of the carbon layer (surface), identified as graphene 2L (d) are depicted on figures 8 (a) through (d) respectively.

For each figure the vertical axis is the total energy in eV *vs* k points in reciprocal space (horizontal axis). Figure 8 (a) provides information regarding energy bands for graphene 2L (a). Notice that a set of multiple degenerate bands cross the Fermi level, which is located at -11.24 eV. Obvious to say, that the system presents a metallic behavior. Figure 8 (b) yields energy bands for graphene 2 L (b). The two carbon atoms were located at 1.64 Å from the lower layer. Notice some differences were encountered when compared with figure 8 (a). The Fermi level was shifted to -11.08 eV with respect to the lower level. Moreover, the system behaves as less metallic due that only two degenerate bands interlaced and cross the Fermi level. The difference could be attributed to the two carbon atoms displaced form the network and intercalated in between the two layers.

In addition, Figure 8 (c) yields information regarding graphene 2L (c). Separation in between two Pd atoms is of the order of 2.84 Å and these two atoms were located at 0.98 Å from the surface. Note that the Fermi level has been displaced to -10.98 eV. Furthermore, the system continues to present metallic behavior like case (b). The difference encountered could be attributed to the interaction of the two Pd atoms with one of the carbon layers. Moreover, figure 8 (d) corresponds to graphene 2L (d). The differences encountered with respect to graphene 2L (a) are the following: The Fermi level was displaced to -10.25 eV while a minigap (between the Valence and Conduction bands) was manifested. The minigap was of the order of ~ 0.02 eV, indicating that the system behaves like a small gap semiconductor. This result implies that the 6 Pd atoms strongly influence the system for changing from metallic to semiconductor behavior. From the calculations described herein, the following conclusions about graphene decorated with Pd atoms can be drawn. The calculated energy bands for graphene 2L(a), graphene 2L (b) and graphene 2L (c) showed metallic behavior, while for graphene 2L (d) yielded a small gap semiconductor.

For each figure the vertical axis is the total energy in eV *vs* k points in reciprocal space (horizontal axis). Figure 8 (a) provides information regarding energy bands for graphene 2L

(a). Notice that a set of multiple degenerate bands cross the Fermi level, which is located at -11.24 eV. Obvious to say, that the system presents a metallic behavior. Figure 8 (b) yields energy bands for graphene 2L (b). The two carbon atoms were located at 1.64 Å from the lower layer. Notice some differences were encountered when compared with figure 8 (a). The Fermi level was shifted to -11.08 eV with respect to the lower level. Moreover, the system behaves as less metallic due that only two degenerate bands interlaced and cross the Fermi level. The difference could be attributed to the two carbon atoms displaced form the network and intercalated in between the two layers.

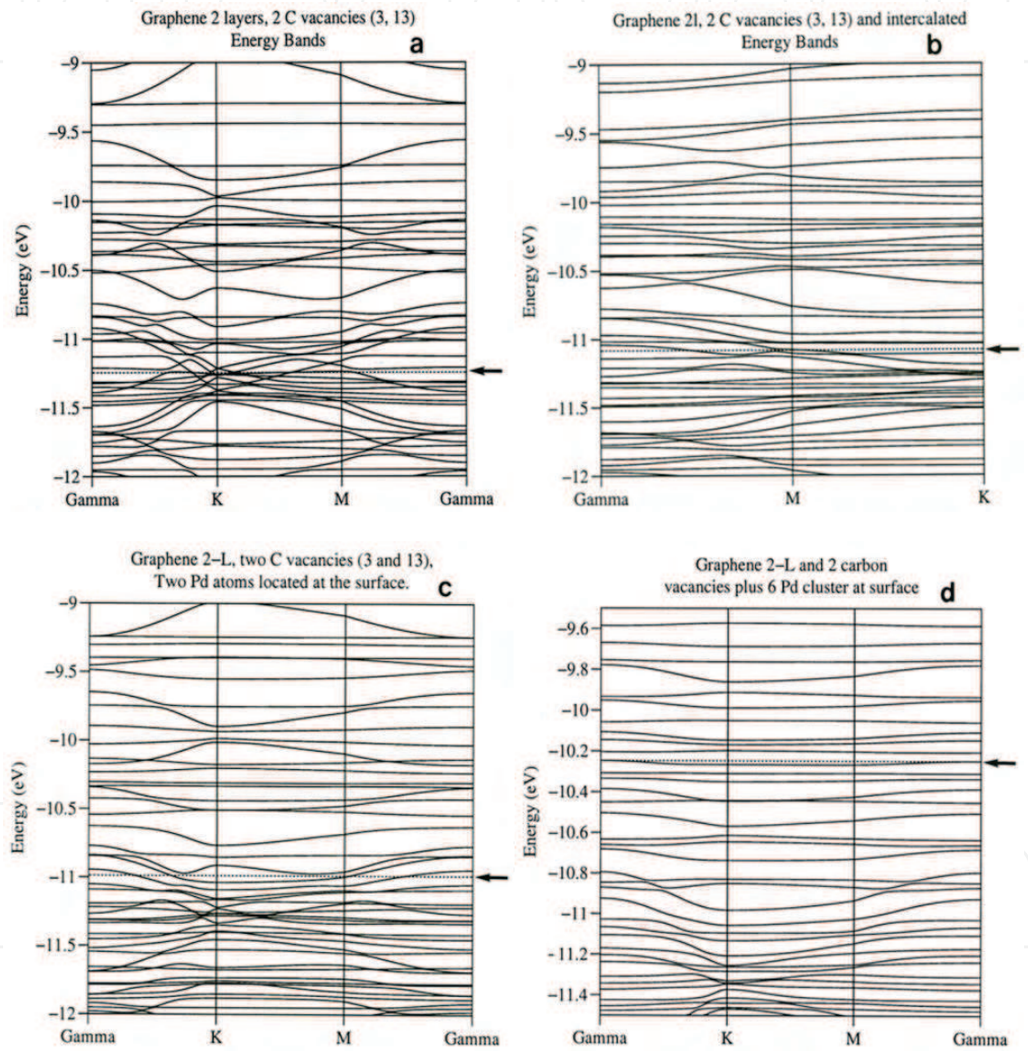

Fig. 8. (a) Graphene two layers with two Carbon vacancies (3 and 13) energy bands. The inset depicts the Wiegner-Seitz cell for a hexagonal configuration. (b) Graphene two layers with two Carbon vacancies (3 and 13) and intercalated in between the two Carbon layers. (c) Graphene two layers with two Carbon vacancies and intercalated inbetween the two Carbon layers with two Pd atoms on the surface layer. (d) Graphene two layers with two Carbon vacancies and intercalated in between the two Carbon layers with 6 Pd atoms on the surface layer.

In addition, Figure 8 (c) yields information regarding graphene 2L (c). Separation in between two Pd atoms is of the order of 2.84 Å and these two atoms were located at 0.98 Å from the surface. Note that the Fermi level has been displaced to -10.98 eV. Furthermore, the system continues to present metallic behavior like case (b). The difference encountered could be attributed to the interaction of the two Pd atoms with one of the carbon layers. Moreover, figure 8 (d) corresponds to graphene 2L (d). The differences encountered with respect to graphene 2L (a) are the following: The Fermi level was displaced to -10.25 eV while a minigap (between the Valence and Conduction bands) was manifested. The minigap was of the order of ~ 0.02 eV, indicating that the system behaves like a small gap semiconductor. This result implies that the 6 Pd atoms strongly influence the system for changing from metallic to semiconductor behavior. From the calculations described herein, the following conclusions about graphene decorated with Pd atoms can be drawn. The calculated energy bands for graphene 2L(a), graphene 2L (b) and graphene 2L (c) showed metallic behavior, while for graphene 2L (d) yielded a small gap semiconductor.

5. Results and discussion

The morphology and size distribution of metallic particles produced by the reduction of metallic salts in solution depends on various reaction conditions such as temperature, time, concentration, molar ratio of metallic salt/reducing agent, mode and order of addition of reagents, presence and type of protective agents, degree and type of agitation, and whether nucleation is homogeneous or heterogeneous [Sanguesa, C. D., et al., 1992].

Following the polyol method with ethylene glycol as solvent reductor, it was possible to obtain monometallic nanoparticles with narrow size distributions in systems and different structures depending on the temperature of reaction. The monometallic synthesis of nanoparticles by itself showed distinctive morphologies of the nanoparticles depending on the temperature of reaction.

Reaction proceeds in general as an oxidation of the ethylene glycol reducing the metallic precursor to its zero-valence state. [Carotenuto, G., et al. 2000; Sun, Y. et al., 2002]

$$OH\text{-}CH_2\text{-}CH_2\text{-}OH \rightarrow CH_3\text{-}CHO + H_2O \quad (1)$$

$$4(CH3-CHO) + H_2PtCl_6 \rightarrow 2(CH_3-CO-CO-CH_3) + Pt^0 + 6HCl \quad (2)$$

This reaction describes the reduction of Pt^{+2} to Pt^0.

$$OH-CH_2-CH_2-OH \rightarrow CH_3-CHO + H_2O \quad (3)$$

$$2(CH_3-CHO) + PdCl_2 \rightarrow (CH_3-CO-CO-CH_3) + Pd^0 + 2HCl \quad (4)$$

This reaction describes the reduction of Pd^{+2} to Pd^0.

In the presence of a surface modifier, the reaction changes depending on the ability of the metal to coordinate with it, as in the case of PVP where the metallic precursor could

coordinate with the oxygen of the pyrrolidone group, when the particles are in the nanometer size range, while when they are in the micrometer size range the coordination is mainly with the nitrogen, as reported by F. Bonet et al.[Sun, Y. et al., 2002; Bonet, F. et al., 2000]

By the polyol method with ethylene glycol as solvent-reductor, was possible to obtain monometallic platinum and palladium Nps with narrow size distributions in systems with small particles (2-4 nm) and different structures depending on the temperature of reaction. The structure of platinum and palladium Nps are cubic, face centered. The monometallic synthesis of Pt and Pd Nps by itself showed a distinctive morphology of quasi hemispherical small Pt and Pd Nps, which does not depend on the temperature of reaction has can be seen from Figure 1 (a) and (b).

The Pt and Pd Nps synthesized by polyol method, were deposited successfully on the HOPG in figure 2 can be seen Pt Nps on HOPG.

In the case when the Pt Nps were synthesized by direct reduction of platinum salt in H_2 flow on HOPG we obtained Nps with a considerable size distributions in systems of Pt Nps and different structures depending on the temperature of reaction. [Tomita &Tamai,1974; Baker et al., 1982]

By immersing the graphite electrode into a platinum plating solution were obtained Pt Nps in a narrow particle size distribution also for mean crystallite diameters smaller than 4 nm.

The formation of small Pd Nps with a uniform distribution over the electrode is achieved fast also by overpotential deposition as in the case of platinum with higher Pd^{2+} concentrations in solution.

It is important to observe that several patterns of diffraction of the samples Pt Nps on HOPG presented rotations of some degrees between the layers of HOPG in the direction perpendicular to the basal plane by effect of heating these samples in H_2. Also Moire patterns were observed in some of these samples. Honeycomb structures were observed on the HOPG surface.

For preparing supported platinum and palladium Nps on HOPG graphite for investigations of electrocatalysis, the advantage of the polyol method is the small size of the particles and the narrow distribution sizes of them. The second method have the potential to yield nanocrystals that are disposed in direct contact with HOPG; however, in neither case has it been possible to achieve good particle size monodispersity for platinum and palladium across a wide range of particle sizes.

Electrochemical deposition resulted an effective method to obtain directly nanoscale platinum and palladium particles on HOPG with a narrow size distribution.

The system remains semi metallic for Pt Nps calculations, except when a cluster of 6 Pt atoms was located on the surface of one of the graphene layers. For this case, the system behaves as a semi conductor with an energy gap $E_g \sim 0.05$ Ev, In most of the cases.

Energy bands were performed and provided information about the metallic behavior in the case of Pd Nps, for the three cases enunciated formerly, showing more metallic character for

the first case, while less metallic behavior for the second one. Moreover, for graphene 2L with vacancies and intercalated with six Pd atoms on the surface showed a mini gap (between the Conduction and Valence Bands) of the order of 0.02 eV and manifesting semiconductor behavior.

6. Conclusions

In all cases, the deposition is sufficiently extensive to bind the Pt and Pd nanoparticles with HOPG and to permit the observation of a crystalline reorganization during the dissipation of the heat into the surroundings. We have been able to explain the original diffraction patterns observed in graphene with Pt atoms decorated on the surface, these are the direct result of a rotation of layers of the carbon honeycomb network.

From the theoretical analysis described herein, the following conclusions about graphene decorated with Pd atoms can be drawn that the graphene shown metallic behavior in some specific cases, which is very important to improve the physicochemical properties of graphene. These conclusions might apply as well to graphite, which also shows a two-dimensional spectrum, carbon nanotubes, which have a similar properties, and other materials with similar electronic structure.

7. Acknowledgment

Authors would like to acknowledge Professor Allen J. Bard, Facultad de Ciencias Físico Matemáticas, PAICYT Project and Microscopy Laboratory of CIIDIT de la Universidad Autónoma de Nuevo León for their support.

8. References

Ahmadi, T. S., Wang, Z. L., Green, T. C., Henglein, A., El-Sayed, M. A. (1996). Shape-Controlled Synthesis of Colloidal Platinum Nanoparticles. *Science,* 272, 1924.

Allongue, P., Souteyrand, E. (1993).*J. Electroanal. Chem.*362, 79.

Alvarez, M. M., Khoury, J. T., Schaaff, G., Shafigullin, M. N., Vezmar, I., Whetten, R. L. (1997). Optical Absorption Spectra of Nanocrystal Gold Molecules.*J. Phys. Chem. B.* 101, 3706.

Alvarez, S. (1993). *Tables of parameters for extended Hückel calculations*. (March 1993), Universitat de Barcelona, Spain.

Amiens, C., de Caro, D., Chaudret, B., Bradley, J. S., Mazel, R.; Roucau, C. (1993). *J. Am. Chem. Soc.* 115, 11638.

Andres, R. P., et al. (1992). Nanostructured Materials Promise to Advance Range of Technologies. *Chem. Eng. News, (*Nov 18, 1992).

Baker, B. E., Kline, N. J., Treado, P. J., Natan, M. J.(1996).*J. American Chemical Society,* 118, 8721.

Baker, R. T., Sherwood, R.S., Derouane, E. O. (1982).*J. Cat.* 75, 382.

Bard, A. J. Photochemistry.*Science. (*1980). 207, 139.

Bartolomew, C. H., Boudart, M. (1972).*J. Catalysis,* 25, 173.

Beyer, H., Müller, M., Schimmel, T. (1999).*Applied Physics A,* Science and Prosessing, Vol. 68, No. 2, pp.0947-8396.

Bonet, F., Delmas, V., Grugeon, S., Herrera-Urbina, R., Silvert, P. Y., Tekaia-Elhsissen, K. (1999). *NanoStruct. Materials.* 11, 1277.

Bonet, F., Tekaia-Elhsissen, K., Sarathy, K. V. (2000). *Bull. Mater. Sci. 23*, 165.

Bradley, J. S., Millar, J. M., Hill, E. W., Behal, S., Chaudret, B., Duteil, A. *(* 1991). Surface Chemistry on Colloidal Metals: Spectroscopic Study of Adsorption of Small Molecules *Faraday Discuss. 92*, 255.

Bradley, J. S.; Hill, E. W.; Behal, S.; Klein, C. (1992). Preparation and characterization of organosols of monodispersed nanoscale palladium. Particle size effects in the binding geometry of adsorbed carbon monoxide.*Chem. Mater.* 4, 1234.

Bronstein, L. M., Chernyshov, D. M., Volkov, I. O., Ezernitskaya, M. G., Valetsky, P. M., Matveeva, V. G., Sulman, E. M. (2000). Structure and Properties of Bimetallic Colloids Formed in Polystyrene-*block*-Poly-4-vinylpyridine Micelles: Catalytic Behavior in Selective Hydrogenation of Dehydrolinalool. *J. Catal.* 196, 302.

Cachet, H., Froment, M., Souteyrand, E., Denning, C.(1992) *J. Elecrochem. Soc.* 139, 2920.

Cao, G. (2004). *Nanostructures and nanomaterials, synthesis, properties and applications*(First Edition). Imperial College Press, England.

Colvin, V. L., Schlamp, M. C., Alivisatos, A. P. (1994). Light-Emitting Diodes Made From Cadmium Selenide Nanocrystals and a Semiconducting Polymer.*Nature,* 370, 354.

Diculescu, V.C., Chiorcea-Paquim, A.M., Corduneanu, O., Oliveira Brett, A.M. (2007). Palladium nanoparticles and nanowires deposited electrochemically: AFM and electrochemical characterization, *J.Solid State Electrochem.* 11, 887-898.

Esumi, K., Matsuhisa, K., Torigoe, K.(1995). Preparation of Rodlike Gold Particles by UV Irradiation Using Cationic Micelles as a Template. *Langmuir.*11, 3285.

Freelink, T., Visscher, W., Van Veen, J. A. R.(1995). *J. Electroanal. Chem.* 382, 65.

Galván, D. H.(1998) Extended Hückel calculations on cubic boron nitride and diamond. *J. Mat. Sci. Lett.*17, 10, 805-810.

Galván, D. H., Posada-Amarillas, A., Elizondo, N., Mejia, S., Pérez-Tijerina E., José-Yacamán, M. (2009). Diffraction Patterns Observed in Two-layered Graphene and Their Theoretical Explanation. *Fullerenes, Nanotubes and Carbon Nanostructures.*17, 258-272.

Galván, D. H., Posada-Amarillas, A., Núñez-González, R., Mejía S., José-Yacamán M. (2010). Study of Vacancies and Pd Atom Decoration on the Electronic Properties of Bilayer Graphene. *Journal of Superconductivity and Novel Magnetism*, 23, 1543-1550.

García Gutiérrez D.I., Gutiérrez-Wing, C. E., Giovanetti, L., Ramallo-López, J. M., Requejo, F. G., José-Yacamán, M.(2005). Temperature Effect on the Synthesis of Au-Pt Bimetallic Nanoparticles. *J. Phys. Chem. B* , 109, 3813-3821.

Glassey, V. W., Papoian, G. A., Hoffmann, R., (1999). The energy partition within one-electron formalism: A Hamiltonean population of study surface-CO interaction in the c(2x2)-CO/Ni (100) chemisorption system. *J. Chem. Phys.* 111, 3, 893-910.

Grabar, K. C., Freeman, R. G., Hommer, M.B., Natan, M. *J.* (1995). Preparation and Characterization of Au Colloid Monolayers. *Anal. Chem.* Vol. 67, No. 4, (February 1995), pp.735-743.

Halperin, W. P. (1986). Quantum Size Effects in Metallic Powders*Rev. Mod. Phys.* 58, 533.

Han, S. W., Kim, Y. Kim, K.,(1998). Dodecanethiol-Derivatized Au/Ag Bimetallic Nanoparticles: TEM,. UV/VIS, XPS, and FTIR Analysis. *J. Colloid Interface Sci.*, 208, 272.

Henglein, A. (1993). Physicochemical properties of small metal particles in solution: "microelectrode" reactions, chemisorption, composite metal particles, and the atom-to-metal transition.*J. Phys. Chem. 97*, 5457.

Henglein, A. (2000). Preparation and Optical Aborption Spectra of $Au_{core}Pt_{shell}$ and $Pt_{core}Au_{shell}$ Colloidal Nanoparticles in Aqueous Solution. *J. Phys. Chem. B*.104, 2201.

Hirai, H. (1979). Formation and catalytic functionality of synthetic polymer noble metal colloid.*J. Macromol. Sci.-Chem. A*, 13, 633.

Hirai, H., Chawanya, H., Toshima, N. (1985). Colloidal palladium protected with poly(*N*-vinyl-2-pyrrolidone) for selective hydrogenation of cyclopentadiene. *React. Polym. 3*, 127.

Hirai, H.; Toshima, (1986) N. *Tailored Metal Catalysts*; Iwasawa, Y., Ed., D. Reidel, Dordrecht, pp 87-140.

Hoffmann, R. (1963).An Extended Hückel theory. I. hydrocarbons. *J. Chem. Phys.* 39, 6, 1397-1412.

Hoffmann, U., Wilm, D. Z. (1936). *Elektrochem.,* 42, 42.

Hull, A. W., (1917). A new method of X-ray crystal analysis, *Phys. Rev.* 10, 6, 661-696.

Kan, C.; Cai, W., Li, C.; Zhang, L., Hofmesiter, H. (2003) *J. Phys. D: Appl. Phys. 36*, 1609.

Katakuse, I. (1994). *J. Mass Spectrom. Soc. Jpn. 42*, 67.

Knight, W. D., Clemenger, K., deHeer, W. A., Saunders, W. A., Chou, M. Y., Cohen, M. (1984). *Phys. Rev. Lett. 52*, 2141.

Leff, D. V., Ohara, P. C., Heath, J. R., Gelbart, W. M. (1995). *J. Phys. Chem.* 99, 7036.

Lewis, L. N. (1993). *Chem. Rev.* (Washington, D.C.) 93, 2693.

Moiseev, I. I. (1995). *J. Mol. Catal. 95*, 109.

Park, H. K.; Lim, Y. T.; Kim, J. K.; Park, H. G.; Chung, B. H. (2008). *Ultramicroscopy* 108,10, 1115.

Pauling, L. (1960). The Nature of the Chemical Bond, p. 235, 3rd. Edition.

Poulin, J. C., Kagan, H. B., Vargaftik, M. N., Stolarov, I. P., Moiseev, I. I. *J. Mol. Catal.* (1995), 95, 109-113.

Reetz, M. T., Helbig, W.(1992).*J. Am. Chem. Society,* 116, 7401.

Reetz, M. T., Winter, M., Tesche, B. *(*1997). *Chem. Commun.* 147.

Sanchez-Ramirez, J. F., Pal, U. (2001). *Superficies Vac. 13*, 114.

Schmid, G. (1988). *Polyhedron,* 7, 2321.

Schmid, G. (1992). *Chem. Rev.* (Washington, D.C.)*92*, 1709.

Schmid, G. (1994).*Clusters and Colloids* (First Edition), Verlagsgesellschaft, *Weinheim,* ISBN 527–29043–5, Germany.

Schmid, G., Giebel, U., Huster, W., Schwenk, A. (1984). *Inorg. Chim. Acta 85*, 97.

Schmid, G., Harms, M., Malm, J.O., Bovin, J.O., van Ruitenbeck, J., Zandbergen, H. W., Fu, W. T.(1993), *J. Am. Chem. Soc.* 115, 2046.

Schmid, G., Morun, B., Malm, J. O. (1989). *Angew. Chem., Int.* Ed. Engl. *28*, 778.

Snow, D., Major, M., Green, L. (1996). *Microelectronic Engr.* 30, 969.

Sugano, S. (1991). *Microcluster Physics*; Springer-Verlag: Berlin.

Sun, Y., Yin, Y., Mayers, B. T., Herricks, T., Xia, Y. (2002). *Chem. Mater. 14,* 4736.

Tekaia-Elhsissen, K., Bonet, F., Silvert, P. T., Herrera-Urbina. R. (1999). *J. Alloys Compounds 292*, 96.

Teranishi, T., Miyake, M. (1998). *Chem. Mater.* 10, 594-600.

Teranishi, T., Hosoe, M., Miyake, M. (1997). *Adv. Mater. 9*, 65.

Teranishi, T., Nakata, K., Miyake, M., Toshima, N. *(*1996). *Chem. Lett.* 277.

Thomas, J. M., Raja, R., Johnson, B. F. G., Hermans, S., Jones, M. D., Khimyak, T.(2003). *Ind. Eng. Chem. Res.* 42, 1563.

Tomita A.,Tamai, Y. (1974).*J. Phys. Chem.,* 78, 2254.

Toshima, N., Harada, M., Yonezawa, T., Kushihashi, K., Asakura, K. (1991). *J. Phys. Chem. 95*, 7448.

Toshima, N., Kuriyama, M., Yamada, Y., Hirai, H. (1981). *Chem. Lett.* 793.

Toshima, N., Takahashi, T. (1992). *Bull. Chem. Soc. Jpn.* 65, 400.

Toshima, N., Wang, Y. (1994). *Adv. Mater.* 6, 245.

Toshima, N., Yamaji, Y., Teranishi, T., Yonezawa, T. *Z. (*1995). *Naturforsch. 50a*, 283.

Turkevich, J.; Stevenson, P.; Hillier, J. (1951). *Discuss. Faraday Soc.* 11, 55.

Vargaftik, N. M.; Moiseev, I. I.; Kochubey, D. I.; Zamaraev, K. I. (1991). *Faraday Discuss. Chem. Soc.* 92, 13.

Viau, G., Toneguzzo, P., Pierrard, A., Acher, O., Fievet-Vincent, F., Fievet, F. (2001). *Scripta Mater.* 44, 2263.

Volokitin, Y., Sinzig, J., de Jong, L. J., Schmid, G., Vargaftik, M. N., Moiseev, I. I. (1996). *Nature,* 384, 621.

Wei-xia, T. *(2008). Chinese Journal of Polymer Science.* 26, 1, 23−29.

Whangbo, M-H., Hoffmann, R. (1978). The band structure of the tetracyanoplatinate chain. J. *Am. Chem. Soc.,* 100 ,19, 6093-6098.

Williams, D. B., Carter, C. B.(1996).*Transmission Electron Microscopy*, Plenum Press, New York.

Willner, I., Maidan, R., Mandler, D., Dürr, H., Dörr, G., Zengerle, K. *(*1987). *J. Am. Chem. Soc.* 109, 6080.

Wolfsberg, M. W.; Helmholtz, L. The spectra and electronic structure of the tetrahedral ions MnO_4^{-1}, CrO_4^{-2}, and $ClO4^{-1}$. (1952). *Chem. Phys.* 20, 5, 837-843.

Yang, D-Q., Zhang, G.-X., Sacher, E. , José-Yacamán, M., Elizondo N. (2006). Evidence of the Interaction of Evaporated Pt Nanoparticles with Variously Treated Surfaces of Highly Oriented Pyrolytic Graphite.*J. Phys. Chem. B*. 110, 8348-8356.

Yonezawa, T., Tominaga, T., Toshima, N. (1995). Novel Characterization of the Structure of Surfactants on Nanoscopic Metal Clusters by a Physicochemical Method. *Langmuir.* 11, 4601.

Yonezawa, T., Toshima, N. (1993). Polymer- and micelle-protected gold/platinum bimetallic systems. Preparation, application to catalysis for visible-light-induced hydrogen

evolution, and analysis of formation process with optical methods. *J. Mol. Catal. 83*, 167.

Zoval, J. V., Lee, J., Gorer, S., Penner, R. M.(1998). Electrochemical preparation of platinum nanocrystallites with size selectivity on basal plane oriented graphite surfaces.*J. Phys. Chem. B,* 102, 1166-1175.

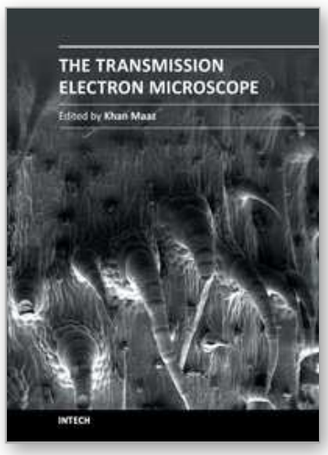

The Transmission Electron Microscope
Edited by Dr. Khan Maaz

ISBN 978-953-51-0450-6
Hard cover, 392 pages
Publisher InTech
Published online 04, April, 2012
Published in print edition April, 2012

The book "The Transmission Electron Microscope" contains a collection of research articles submitted by engineers and scientists to present an overview of different aspects of TEM from the basic mechanisms and diagnosis to the latest advancements in the field. The book presents descriptions of electron microscopy, models for improved sample sizing and handling, new methods of image projection, and experimental methodologies for nanomaterials studies. The selection of chapters focuses on transmission electron microscopy used in material characterization, with special emphasis on both the theoretical and experimental aspect of modern electron microscopy techniques. I believe that a broad range of readers, such as students, scientists and engineers will benefit from this book.

INTECH
open science | open minds

InTech Europe
University Campus STeP Ri
Slavka Krautzeka 83/A
51000 Rijeka, Croatia
Phone: +385 (51) 770 447
Fax: +385 (51) 686 166
www.intechopen.com

InTech China
Unit 405, Office Block, Hotel Equatorial Shanghai
No.65, Yan An Road (West), Shanghai, 200040, China
中国上海市延安西路65号上海国际贵都大饭店办公楼405单元
Phone: +86-21-62489820
Fax: +86-21-62489821

IntechOpen